BPES-Related Mathematical Development for the Phase Shift Due to Rf Magnetic Field in Heart Inferior Coronary Artery NMR Imaging

Awojoyogbe OB[1], Boubakker karemt [2]*, Aweda MA[3] and Dada M[1]

[1]Department of Physics, Federal University of Technology, Minna, Niger-State, Nigeria
[2]Unite de Physique de Dispositifs a Semiconducteurs -UPDS- Faculte des Sciences de Tunis, Campus Universitaire 2092 Tunis, Tunisia
[3]Department of Radiation Biology and Radiotherapy, College of Medicine of the University of Lagos. Idi-Araba, P. M. B. 12003, Lagos State, Nigeria

Abstract

It is known that most cardiovascular emergencies are caused by coronary artery disease. Nevertheless, in the last decade's related literature, data about mathematical models of heart and heart vessels along with NMR/MRI features is not accordingly abundant. In fact there are inherent difficulties in developing this type of mathematical models to completely describe the real or ideal geometries of heart arterial system. In this study, a mathematical formulation for the NMR diffusion partial differential equation derived from the Bloch NMR flow equations to describe in detail the activities in lower heart coronary artery is presented. Based on the Bloch NMR flow equations, we deduce analytical expressions to describe in detail the NMR transverse magnetizations and signals as a function of some NMR flow and geometrical parameters which are invaluable for the analysis of blood flow in heart vessels. The boundary conditions are inherently introduced based on the properties of the Boubaker polynomials expansion scheme BPES.

Keywords: Bloch NMR flow equations; NMR diffusion equation; Heart vessels; Coronary artery; Functional magnetic resonance imaging fMRI; Boubaker Polynomials Expansion Scheme (BPES)

Introduction

Phase contrast technique employs the phase shift in the MR signal that is induced by the flowing blood in heart vessels. The merit of investigations on MR signals in heart disease treatments, heart tomographic imaging and discrimination between infracted, ischemic or normal myocardium has been early highlighted during the last decades through the works i.e. of Berman et al. [1,2] and Ingwall [3]. More recently, confirmation of accuracy and efficiently have been reported by several studies [4-8]. In this technique setup, blood spins moving along an applied gradient acquire a phase shift which is proportional to the strength and the duration of the gradient and the motion of the spins. In other terms, by applying two gradients, equal in duration and steepness but opposite polarity called bipolar gradients, a moving spin during the time the gradient is on, will either gain or lose a phase shift due to the motion in the increasing or decreasing magnetic field. This phase shift is proportional to the velocity of the moving spins, as long as the velocity of the spins is constant [9-11]. Thus the phase signal of stationary spins will be zero and this means that small heart arteries can be visualized, even with slowly moving blood. The phase shift of moving spins will be proportional to their constant velocity. The phase shift due to higher order motions, for example, acceleration, pulsation, etc, can be neglected under normal physiological condition. The errors of ignoring the higher order motions can be minimized by using short echo times (TE) especially in distributed flow.

Methods

The MRI signal at the sampling time t_s, induced by spin at the position $r(t_s)$ which is excited by a slice selective radio frequency pulse given by:

$$S(\vec{r}, t_s) = \gamma \int_{t_1}^{t} e^{i\theta(\vec{r}, t_s)} dt \qquad (1)$$

The phase $\theta(\vec{r}, t_s)$ of the MRI signal is:

$$\theta(\vec{r}, t_s) = \int_{t_1}^{t} \omega(\vec{r}, t) dt \qquad (2)$$

The Larmor frequency $\omega(\vec{r}, t)$ $\omega(\vec{r}, t)$ and the main magnetic field $B(\vec{r}, t)$ are usually defined respectively as:

$$\left.\begin{array}{l} \omega(\vec{r}, t) = \gamma B(\vec{r}, t) \\ B(\vec{r}, t) = B_0 + \vec{r}(t)\, \vec{G}(t) \end{array}\right\} \qquad (3)$$

Where B_0 is the static magnetic field, $\vec{r}(t)$ is the spatial position and t_1 is the time when spins are excited. By substitution of Eq. (1) into Eq. (2), the phase of the MRI signal becomes:

$$\theta(\vec{r}, t_s) = \gamma \int_{t_1}^{t} \left[B_0(r) + \vec{r}(t)\vec{G}(t) \right] dt \qquad (4)$$

Since $\vec{r}(t)$ is not constant for moving spins, $\vec{r}(t)$ can be approximated in Eq. (4) by Taylors series as follows:

$$\theta(\vec{r}, t_s) = \gamma B_0(\vec{r}_0)(t_s - t_1) + \gamma \vec{r}_0 \int_{t_1}^{t} \vec{G}(t)dt + \gamma \vec{v}_0 \int_{t_1}^{t} \vec{G}(t)tdt + \frac{1}{2}\gamma \vec{a}_0 \int_{t_1}^{t} \vec{G}(t)t^2 dt + \cdots \qquad (5)$$

Where $r_0 = r(t_0)$: Position of spins, $v_0 = v(r, t_0)$: Blood flow velocity, $a_0 = a(r, t_0)$: Blood flow acceleration (or deceleration) and γ = the gyro magnetic ratio of the hydrogen nucleus.

By setting a mono dimensional system, considering spatial dependence and setting a dimensionless time variable $\tilde{t}$:

$$\tilde{t} = \frac{2t - t_1 - t_s}{t_s - t_1} \qquad (6)$$

We have:

$$\theta(x) = u(x) + \int_{-1}^{1} \Omega(x,\tilde{t})\theta(\tilde{t})d\tilde{t} \tag{7}$$

Where θ is the phase shift to be determined and $\Omega(x,\tilde{t})$ is a pondering function defined, conjointly with the given function $u(x)$, according to the system geometry (Figure 1).

The first term (the constant term) in Eq. (5) is induced by the main magnetic field $\vec{B}_0$ and does not affect the reconstructed image. From the second term (the spatial term) the localization of the MRI signal is derived. The third term, also called the velocity term, contains the information about the instantaneous velocity of the spins. A careful estimation for the axial velocity component shows that the acceleration and the higher order terms can be neglected as long as the local acceleration of the blood flow remain physiological. On another hand, several magnetic resonance (MR) techniques have been based on the linearity between phase angle and velocity of moving blood in a gradient field as demonstrated by Meier et al. [12] , Bogren et al. [13,14] and Stahlberg et al. [15].

It is observed that the second term in Eq. (5) represents the phase shift due to the effects of the rF magnetic field. Traditionally, in any magnetic resonance imaging system we can consider the normalized magnetic field created conjointly by two similar circular coaxial conducting magnetic coils of radius R_0, separated by a distance $\varpi \times R_0$ (Figure 1), where ϖ is a positive real parameter. In this position NMR sensitive region is concentrated on the heart muscle along with the lower part of either inferior vena cava or lower coronary artery (according to field direction). For this geometry, we have [16-17]:

$$\begin{cases} \Omega(x,\tilde{t}) = \dfrac{\varpi}{\varpi^2 + (x-\tilde{t})^2} \\ u(x) = kx, \quad k \in \left]-\infty;+\infty\right[\end{cases} \tag{8}$$
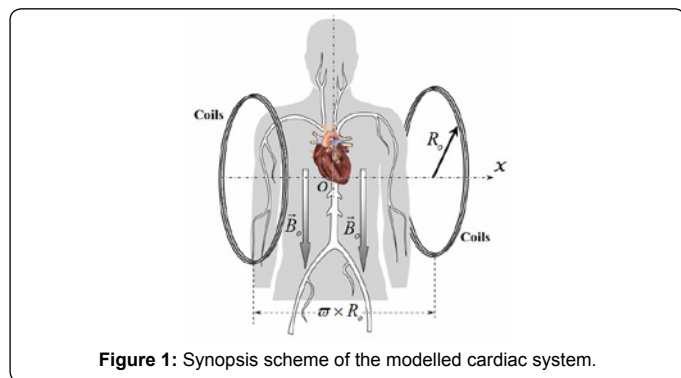

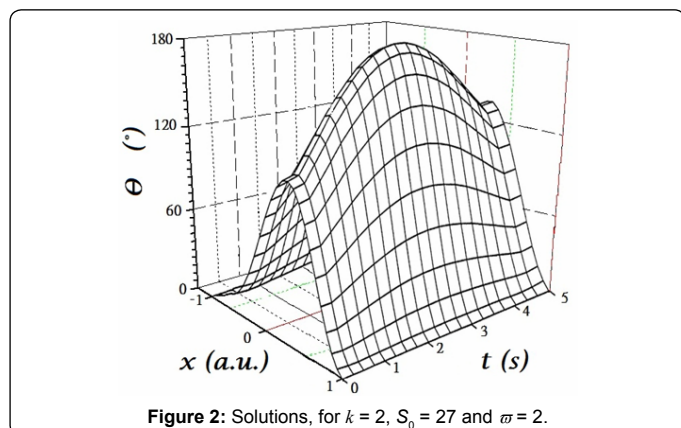**Figure 1:** Synopsis scheme of the modelled cardiac system.

Figure 2: Solutions, for $k = 2$, $S_0 = 27$ and $\varpi = 2$.

Results and Discussion

The proposed resolution protocol *BPES* begins by expressing phase shift $\theta(x)$ as a polynomial expansion:

$$\theta(x) = \sum_{m=1}^{+\infty} \beta_m . B_{4m}(x) \tag{9}$$

Truncated, as a physically accepted weak solution to:

$$\theta(x) = \sum_{m=1}^{S_0} \beta_m . B_{4m}(x) \tag{10}$$

Where $B_{4m}(x)$ are the 4m-order Boubaker polynomials (18-30), β_m are unknown coefficients and S_0 is a given integer.

By introducing Eq. (10) in Eq. (7), one obtains:

$$\sum_{m=1}^{S_0} \beta_m . B_{4m}(x) = u(x) + \int_{-1}^{+1} \frac{\varpi}{\varpi^2 + (x-\tilde{t})^2} \sum_{m=1}^{S_0} \beta_m . B_{4m}(\tilde{t})d\tilde{t} \tag{11}$$

This is simplified to:

$$\begin{cases} \sum_{m=1}^{S_0} \beta_m \left[1 - H_m(x)\right] \times B_{4m}(x) = f(x) \\ H_m(x) = \varpi \int_{-1}^{+1} \dfrac{B_{4m}(\tilde{t})}{\varpi^2 + (x-\tilde{t})^2} d\tilde{t} \end{cases} \tag{12}$$

First, $H_m(x)\big|_{m=1..S_0}$ are calculated using the Boubaker polynomials properties detailed elsewhere [20-26] and in APPENDIX, then Eq. (11) is solved by determining the set $\beta_m^0(x)\big|_{m=1..S_0}$ which minimises the positive difference amount A:

$$A = \left(\sum_{m=1}^{S_0} \beta_m^0 \left[1 - H_m(x)\right] \times B_{4m}(x) - f(x)\right)^2 \Bigg|_{x \in \left]\frac{-\varpi R_0}{2}, \frac{\varpi R_0}{2}\right[}$$

The solutions obtained in the particular case of $k = 2$, $S_0 = 27$ and $\varpi = 2$.

It could be noticed, in Figure 2, that the maximum phase shift is recorded in the central zone which corresponds to heart location, while at edges, where the tissue is absent, the phase shift is totally absent. This result in is in good agreement with the results proposed earlier by Johntson et al. [31], Chan et al. [32], Lethimonnier et al. [33] and Liu et al. [34].

On another hand, it is known that normal heart tissue NMR relaxation times are approximately T_1=570 ms and T_2=57 ms. Since malignant tissues showed higher values of T_1 than normal tissue of same type, it is expected that phase shift profiles differ significantly between normal and i.e. ischemic heart. An appropriate NMR mapping, using the actual results along with those presented in the last decade's literature (31-40) can yield good comparison patterns for identifying heart failure causes.

Conclusion

A solution to NMR diffusion partial differential equation derived from the Bloch NMR flow equations in a model of heart inferior coronary artery has been presented. Based on the Bloch NMR flow equations, we deduce analytical expressions to describe in detail the NMR transverse magnetizations and phase shift as a function of some NMR flow and geometrical parameters which are invaluable for the analysis of blood flow in heart vessels. The boundary conditions are inherently introduced based on the properties of the Boubaker polynomials expansion scheme BPES.

The most important conclusion to draw from the results of this mathematical formulation is that the NMR signal phase shift

evaluation can be very a reliable guide to obtaining basic structural information on the heart dysfunction or anatomic defects.

Acknowledgement

References

1. Berman E, Olivson A, Przyblski (1997) Application of warm cardioplegia early in reperfusion resuscitates the ischemic rat heart. A 13P-NMR study Exp Ciln Cardiol 2: 184-190.

2. Berman E, Chandra M, Olivson A, Uretzky G, Borman JB, Atlan H, et al. (1995) Myocardial protection by warm blood cardioplegia. A 13P nuclear magnetig resonance spectroscopy study of an isolated perfused rat heart. Minerva Cardioangiol 43: 177-183.

3. Ingwall JS (1982) Phosphorous nuclear magnetic resonance spectroscopy of cardiac and skeletal muscles, Am J Phusiol 242: H729-H44.

4. Nakae I, Mitsunami K, Matuo S, Inubushi T, Morikawa S, et al. (2005) Detection of calf muscle alterations in patients with chronic chronic heart failure by 13P magnetic resonance spectroscopy: Impaired adaptation to continuous exercise. Exp Clin Cardiol 10: 4-8.

5. Raman S V, Simonetti O P (2009) The CMR Examination in Heart Failure. Heart Failure Clinics 5: 283-300.

6. Siegel JM Jr, Oshinski JN, Pettigrew RI, Ku DN (1996) The accuracy of magnetic resonance phase velocity measurements in stenotic flow. J of Biomechanics 29: 1665-1672.

7. Videlefsky N, Parks WJ, Oshinski J, Hopkins KL, Sullivan KM, et al. (2001) Magnetic resonance phase-shift velocity mapping in pediatric patients with pulmonary venous obstruction. J of the Am College of Cardiology 38: 262-267.

8. Lethimonnier F, Furber A, Morel O, Geslin P, L'Hoste P, et al. (1999) Three-dimensional coronary artery MR imaging using prospective real-time respiratory navigator and linear phase shift processing: comparison with conventional coronary angiography. Magn Reson Imaging 17: 1111-1120.

9. Scott WA (2008) Magnetic Resonance Imaging of the Brain and Spine, Vol. 1, Lippincott Williams & Wilkins, Chicago, IL.

10. Helle M, Norris DG, Rüfer S, Alfke K, Jansen O, et al. (2010) Superselective pseudocontinuous arterial spin labeling. Magnetic Resonance in Medicine 64: 777-786.

11. Galvosas P, Callaghan PT (2006) Fast magnetic resonance imaging and velocimetry for liquids under high flow rates. Journal of Magnetic Resonance 181: 119-125.

12. Meier D, Maier S, Bosiger P (1988) Quantitative flow measurements on phantoms and on blood vessels with MR. Magn Reson Med 8: 25-34.

13. Bogren HG, Underwood SR, Firmin DN, Mohiaddin RH, Klipstein RH, et al. (1988) Magnetic resonance velocity mapping in aortic dissection. Br J Radiol 61: 456-462.

14. Bogren HG, Mohiaddin RH, Klipstein RK, Firmin DN, Underwood RS, et al. (1989) The function of aorta in ischemic heart disease: a magnetic resonance and angiographic study of aortic compliance and blood flow patterns. Am Heart J 118:234-47.

15. Ståhlberg F, Mogelvang J, Thomsen C, Nordell B, Stubgaard M, et al. (1989) A method for quantification of flow velocities in blood and CSF using interleaved gradient echo pulse sequences. Magn Reson Imaging 8: 655-667.

16. Liang F, Lin F (2010) A fast numerical solution method for two dimensional Fredholm integral equations of the second kind based on piecewise polynomial interpolation. Applied Math and Comp 216: 3073-3088.

17. Miyata A, Hiroyuki Tominaga H, Nagai M (2010) Active site distribution analysis of hydrodenitrogenation catalyst using Fredholm integral equation Applied Catalysis A: General 374: 150-157.

18. Oyodum OD, Awojoyogbe OB, Dada M, Magnuson J (2009) On the earliest definition of the Boubaker polynomials Eur Phys J Appl Phys 46: 21201-21203.

19. Awojoyogbe OB, Boubaker K (2008) A solution to Bloch NMR flow equations for the analysis of homodynamic functions of blood flow system using m- Boubaker polynomials. Curr Appl Phys 9: 278-283.

20. Ghanouchi J, Labiadh H, Boubaker K (2008) An Attempt to solve the heat transfer equation in a model of pyrolysis spray using 4q-order Boubaker polynomials. Int J Heat Technol 26: 49-53.

21. Slama S, Bouhafs M, Ben Mahmoud KB, Boubaker A (2008) Polynomials solution to heat equation for monitoring A3 point evolution during resistance spot welding. Int J Heat Technol 26: 141-146.

22. Slama S, Bessrour J, Bouhafs M, Ben Mahmoud K B (2009) Numerical distribution of temperature as a guide to investigation of melting point maximal front spatial evolution during resistance spot welding using Boubaker polynomials. Numer Heat Transfer PartA 55: 401-408.

23. Slama S, Boubaker K, Bessrour J, Bouhafs M (2009) Study of temperature 3D profile during weld heating phase using Boubaker polynomials expansion. Thermochim Acta 482: 8-11.

24. Fridjine S, Amlouk M (2009) A new parameter: an ABACUS for optimizing functional materials using the Boubaker polynomials expansion scheme. Mod Phys Lett B 23: 2179-2182.

25. Tabatabaei S, Zhao T, Awojoyogbe O, Moses F (2009) Cut-off cooling velocity profiling inside a keyhole model using the Boubaker polynomials expansion scheme. Heat Mass Transfer 45: 1247-1251.

26. Zhao TG, Wang YX, Ben Mahmoud KB (2008) Limit and uniqueness of the Boubaker-Zhao polynomials imaginary root sequence. Int J Math Comput 1: 13-16.

27. Belhadj A, Onyango O, Rozibaeva N (2009) Boubaker polynomials expansion scheme-related heat transfer investigation inside keyhole model. J Thermo-phys Heat Transfer 23: 639-640.

28. Ghrib T, Boubaker K, Bouhafs M (2009) Investigation of thermal diffusivity-microhardness correlation extended to surface-nitrured steel using Boubaker polynomials expansion. Mod Phys Lett B 22: 2893-2907.

29. Guezmir N, Ben Nasrallah T, Boubaker K, Amlouk M, Belgacem S (2009) Optical modeling of compound CuInS2 using relative dielectric function approach and Boubaker polynomials expansion scheme BPES. J Alloys Compd 481: 543-548.

30. Dubey B, Zhao TG, Jonsson M, Rahmanov H (2010) A solution to the accelerated-predator-satiety Lotka-Volterra predator-prey problem using Boubaker polynomial expansion scheme. J Theor Biology 264: 154-160.

31. Johnston DL, Homma S, Liu P, Weilbaecher DG, Rokey R, et al. (1988) Serial changes in nuclear magnetic resonance relaxation times after myocardial infarction in the rabbit: relationship to water content, severity of ischemia and histopathology over a six-month period. Magn Reson Med 8: 363-379.

32. Chan PC, Liu P, Cronin C, Heathcote J, Uldall R, et al. (1992) The use of nuclear magnetic resonance imaging in monitoring total body iron in hemodialysis patients with hemosiderosis treated with erythropoietin and phlebotomy. Am J kidney Dis 19: 484-489.

33. Lethimonnier F, Furber A, Morel O, Geslin P, L'Hoste P, et al. (1999) Three-dimensional coronary artery MR imaging using prospective real-time respiratory navigator and linear phase shift processing: comparison with conventional coronary angiography. Magn Reson Imaging 17: 1111-1120.

34. Liu P, Johnston DL, Brady TJ, Lutrario DM Okada RD (1989) The alterations of magnetic resonance relaxation parameters in excised myocardial tissue during NMR spectroscopy: the effects of time, environmental exposure and TTC staining. Maag Reson Imaging 7: 109-113.

35. Duerk JL, Simonetti OP, Hurst GC, Finelli DA (1994) Experimental Confirmation of Phase Encoding of Phase Encoding of Instantaneous Derivatives of Position. Magn Reson Med 32: 77-87.

36. Wendt RE, Wong WE (1992) Nuclear Magnetic Resonance Velocity Spectral of Pulsatile Flow in a Rigid Tube. Magn Reson Med 27: 214-225.

37. Frayne R, Holdsworth D, Gowman L, Rickey D, Drangova M, et al. (1992) Computer- Controlled Flow Simulator for MR Flow Experiments. J Magn Reson Imaging 2: 605-612.

38. Scheidegger MB, Maier SE, Boesiger P (1992) FID-acquired-echos (FAcE): a short echo time imaging method for flow artefact suppression. Magn Reson Imaging 9: 517-534.

39. Boesiger P, Scheidegger MB, Maier SE, Liu K, Maier D (1992) Visualization and quantification of the human blood flow by magnetic resonance imaging J Biomed Engin 25: 55-56.

40. Mohiaddin RH, Wann SL, Underwood R, Firmin DN, Rees S, et al. (1990) Vena caval flow: assessment with cine MR velocity mapping. Radiolog 177: 537-541.